Atmospheric Environment Vol. 16, No. 12, pp. 2763–2776, 1982
Printed in Great Britain.

0004–6981/82/122763–14 $03.00/0
Pergamon Press Ltd.

MEASURING AND MODELING THE TRANSPORT AND DISPERSION OF kRYPTON-85 1500 km FROM A POINT SOURCE

ROLAND R. DRAXLER

National Oceanic and Atmospheric Administration, Air Resources Laboratories, 6010 Executive Blvd, Rockville, MD 20852, U.S.A.

(*First received* 11 *December* 1981 *and in final form* 23 *February* 1982)

Abstract—The 1974 long-range dispersion experiment in which Kr-85 was released from the Idaho National Engineering Laboratory and sampled twice-daily at 13 locations in the midwestern U.S. was considered inconclusive because very few distinct plumes were observed during the two month experimental period. These data have been reanalyzed and compared with model-calculated concentrations after filtering undesired noise by using the coherence of the measured and calculated air concentration time series as a weighting function.

The dispersion model, which is responsive to the effects of wind shear, performed exceptionally well at the more southern samplers in Oklahoma and Kansas. At the northern sites the Kr-85 from Idaho was masked by fluctuations in background concentration as well as small local sources, both of which produced concentration fluctuations of similar magnitude to the Idaho source. Further, the transport of Kr-85 from Idaho to the northern samplers involved more complicated meteorological regimes than could be accounted for by a simple Lagrangian transport model.

1. INTRODUCTION

It can be stated, without qualification, that no data of sufficient quantity exist in the literature which may be used to verify the meteorological aspects of long-range transport and dispersion models without also modeling the complications of chemical reactions and deposition. Most of the available data were discussed in numerous papers presented at the International Symposium on *Sulfur in the Atmosphere*.

Suitable inert tracers for long-range transport experiments are currently under development. A demonstration experiment (Ferber *et al.*, 1981), consisting of a single 3 h release with 3 h sampling durations at 39 locations over a 75° arc 600 km downwind, showed that the meteorology of long-range transport contains many complications that are only partially understood. From the single release in the afternoon, tracer was observed (on and off) for 3 days along the sampling arc. Although a better understanding of the processes affecting long-range transport can best be attained by analyzing individual episodes, a greater quantity of data are needed to verify the calculations of a particular model.

The most comprehensive long-range transport and dispersion experiment to date used inert Krypton-85 released from the fuel reprocessing plant at the Idaho National Engineering Laboratory. Air concentrations were measured as twice-daily averages over the midwestern U. S. from 25 January to 4 May, 1974. The first month of sampling (sites shown in Fig. 1) provided background data as there were no emissions. During the emission period the Kr-85 plume had no discernible effect on the mean concentration (13.8 pCi m^{-3}). A larger mean (by 0.2 pCi m^{-3}) during the non-emission period was attributed to seasonal variations in the background concentration. Calculations with a long-range transport and dispersion model (Heffter *et al.*, 1975) indicated that the plume would produce peak concentrations about 25% above background at the sampling sites. Very few measured samples showed Kr-85 concentrations to be more than 5% above background.

These Kr-85 air concentration data will be shown to contain plumes that can be attributed to the Idaho source, although the amplitudes at best are only a few per cent above background. Standard linear regression techniques will be applied to the calculated and measured data to indicate the level of model performance. However, even the best model will tend to give low correlations when individual values are compared due to the inherent variability in atmospheric dispersion processes. The low correlations result in biased estimates of the slope of calculated to measured concentrations, which makes the diagnostic analysis of model performance more difficult. The model may calculate average concentration correctly yet, because of the low correlation, the slope would suggest a bias in model calculations that does not exist. For most other air concentration data, where plumes can be easily distinguished from background, this would not be a problem since we could compute average air concentrations with little error.

The complications involved in the use of these data because only small amplitude Kr-85 plumes were measured can be minimized by assuming that the

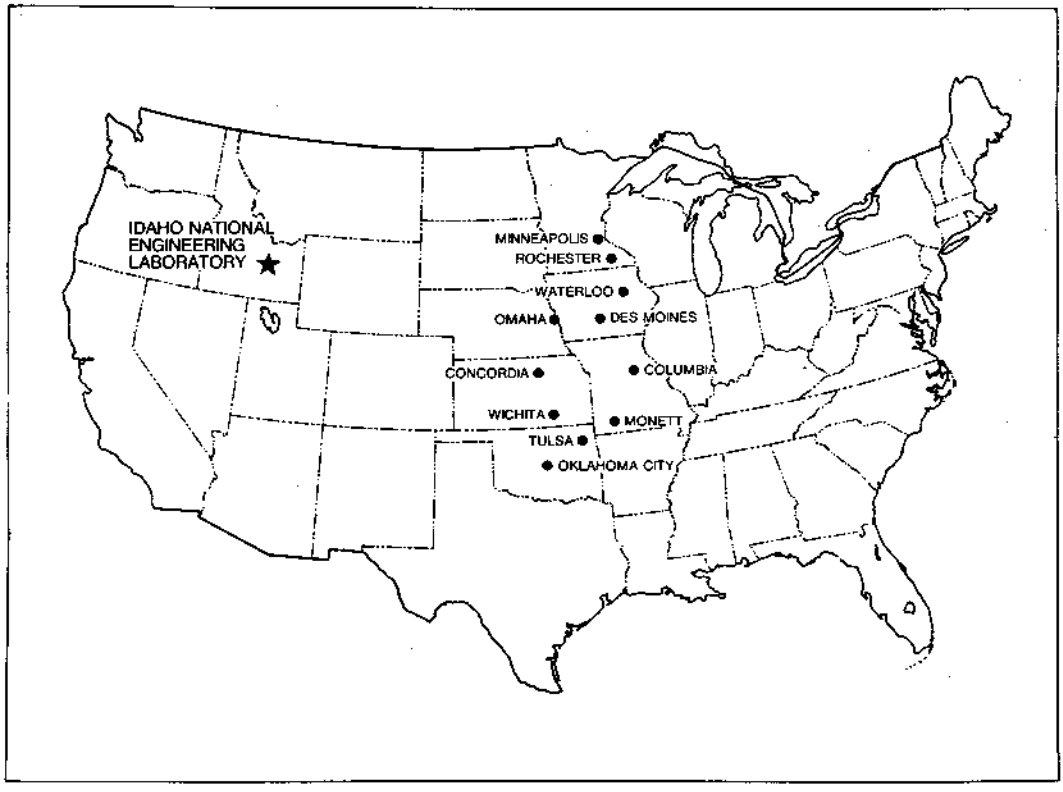

Fig. 1. Map of source location and sampling sites.

concentration data are not just a collection of independent points but a time series with some autocorrelation due to atmospheric turbulence and diffusion. The variation of concentration with time, however small, could have some significance. Therefore, the calculated and measured concentration data will first be filtered to remove noise by using the coherence of the two time series as a filter as each series is reconstructed from its sine and cosine components. In this way uncorrelated fluctuations in the data will be minimized and the linear regression correlations (and slope estimate) should be improved.

The computer model that is used to calculate the concentrations at the sampling sites simulates the effects of wind shear on a pollutant puff. Incorporating the wind shear in long-range dispersion calculations will be shown to compensate for the overcalculations that were found by Ferber *et al.* (1977).

2. THE Kr-85 DATA

The midwest Kr-85 experiment, although comprehensive in scope, has not been extensively utilized. The fact that distinct plumes were not apparent in the data indicates that certain classes of long-range models may consistently overpredict concentrations at these distances (1500 km). This could have significant impact on environmental studies dependent on these models.

Problems with the initial analyses discouraged further use of these data. Variations in background were as large as suspected plumes from Idaho. These variations coincided with airmass changes, polar air having a higher background. A local source was suspected near the northernmost sampler, Minneapolis. The effect of these problems will be discussed further in Section 5.

The details of the sampling and laboratory analysis method were outlined by Ferber *et al.* (1977). Thirteen cryogenic air samplers were installed at NOAA's National Weather Service stations in the midwest to collect two 10 h samples each day (0900–1900 LDT and 2100–0700 LDT, Local Daylight Time). Eleven stations (see Table 1) were located about 1500 km from the source. Two additional samplers were situated at Indianapolis and Detroit (2500 km). However, no

Table 1. Sampling sites and abbreviations

Station	Call letters
Minneapolis, Minnesota	MSP
Rochester, Minnesota	RST
Waterloo, Iowa	ALO
Des Moines, Iowa	DSM
Omaha, Nebraska	OMA
Concordia, Kansas	CNK
Columbia, Missouri	COU
Wichita, Kansas	ICT
Monettt, Missouri	UMN
Tulsa, Oklahoma	TUL
Oklahoma City, Oklahoma	OKC

plumes from Idaho were detected at these more distant sites. Occasional high concentrations at these two sites were attributed to another source and these cases were analyzed by Pack *et al.* (1978).

The Kr-85 emissions from Idaho were through a 76 m high stack (43.59 N, 112.93 W). The 3 h emissions in curies (Ci) are given in Table 2 only for the days when there were emissions. The Kr-85 concentrations in $pCi\,m^{-3}$ are given in Table 3 for the sites listed in Table 1. The values are the concentrations in units and tenths in excess of 12 $pCi\,m^{-3}$. During the first month of sampling, there were no emissions from Idaho. Model calculations for the emission period were performed for 132 consecutive samples starting with the evening sample of local day 57 (26 February sample starting 2100).

Table 2. Three hour emissions of Kr-85 in curies

Day	00Z	03Z	06Z	09Z	12Z	15Z	18Z	21Z
58	0	0	6	180	251	188	184	202
59	4	0	0	0	0	13	181	172
60	153	232	260	135	0	0	0	160
61	214	214	214	214	214	214	200	0
62	0	0	100	200	200	200	200	200
63	200	200	130	0	0	3	269	266
64	314	169	345	76	0	0	0	0
72	0	7	166	255	243	462	162	0
73	0	190	386	437	253	29	0	15
74	252	338	286	369	316	227	0	0
78	0	0	0	47	240	370	318	268
79	50	0	0	0	0	63	391	339
80	424	328	0	0	0	0	0	0
81	54	545	284	419	207	0	0	155
82	242	254	233	294	19	0	0	0
83	0	211	252	348	427	84	0	0
87	0	0	0	0	0	80	280	280
88	280	280	140	0	0	0	0	8
89	220	360	379	336	126	20	0	0
90	0	0	216	266	314	390	184	0
91	0	0	172	345	315	386	152	0
92	0	0	48	290	226	298	352	151
93	0	0	46	300	126	297	331	229
94	0	0	0	0	0	0	0	86
95	359	354	470	154	0	0	0	0
97	0	0	28	330	66	203	175	186
98	175	231	212	4	0	0	0	77
99	331	253	270	408	42	0	0	0
100	0	36	179	453	354	253	174	0
101	0	0	0	7	163	226	288	248
102	132	0	107	177	263	20	0	12
103	66	53	359	263	146	237	197	183
104	18	0	0	0	53	229	212	174
105	161	225	242	148	0	0	0	0
106	40	90	232	314	263	145	139	209
107	150	8	0	0	0	0	0	14
108	115	231	183	240	325	311	15	22
109	141	18	295	478	399	251	233	199
110	282	45	0	0	48	177	242	300
111	229	213	335	62	2	4	6	91
112	215	278	165	202	176	253	94	15
113	14	6	37	1255	290	126	168	21
114	17	10	8	0	38	95	156	209
115	186	57	30	7	50	91	11	196
116	238	26	17	132	83	20	39	36
117	22	71	153	24	166	151	65	0
118	0	13	92	225	65	295	213	206
119	222	158	160	22	2	6	10	10
120	5	5	14	42	100	102	176	148
121	135	213	189	198	163	81	15	12
122	420	395	222	113	123	184	151	190
123	199	191	176	37	0	28	46	11
124	19	137	173	120	60	82	163	148
125	25	110	178	104	9	26	26	113

Days and hours in G.M.T. of beginning time of emission. Days with no emissions are not listed.

Table 3. Measured Kr-85 concentrations given in units and tenths excess from 12 pCi m^{-3}

Local	Morning samples											Evening samples										
day	OK	TU	UM	IC	CO	CN	OM	DS	AL	RS	MS	OK	TU	UM	IC	CO	CN	OM	DS	AL	RS	MS
25		17	15	14		15	16	13	16	15	13	13	14	12	14		15	13	14	17	13	13
26	12	13	12	12		17	13		15	19	13	16	10	12	16	17	16	16	17	18	18	19
27		13	12	14	15	14	12		18	16	17	13	12	17		17	16	16	16		16	17
28		9	14	12	12	15	14	16	15	15	15	10	12	10	12	16	13	14	15	17	15	16
29		7	12	14	12	15	13	15	15	14	18	7	11	12		16	11	10	15	14	16	15
30		7	11	7	11	10	8	11	12	12	14	11	11	12	11	15	8	14	14	15	15	13
31		10	12	14	13	13	14	14	15	14	16	10	13	7	17	9	14	14	13	13	13	
32	8	9	11	13		14	13	19	17	16	16	11	12	13	17	15	13	15	15	19	16	16
33		19	6	6		5	12	16	15	15	14	7	6	11	16	13	9	13	16	18	15	16
34	15	13	12	15	14	15	15	15	16		37	14	9	12	17		16	29	16	16	13	42
35	10	6	7	14	8	8	9	14	13	31	36	8	11	14	12	14	15	13	16	29	29	14
36	12	13	13	11	13	18	12	23	13	13	26	19	5	15	23	17	14	26	14	22		14
37	23	6	24	25	21	26	6	18	10	19	19	24	20	19	25	19	25	20		18	15	29
38	23	6	19	23	21	24	6	19	13	15	16	6	18	19	23	21	22	5	8	22	27	13
39		20	20	15	20		11	17	10	26	14	12	15	17	11	19	12	9	13		15	14
40	14	6	14	14	19	8	17	17	8	24	27	6	14	15	14	16		13	7		16	11
41		12	13	11	14		15	16		21	24	12		14	12	18	13	16	17		21	21
42	11	13	12	12	14	8	13	11	17	13	13	13			12		9	10	10	12	14	13
43	10	10	11	9	12	8	10	8	9	13	10	8	11		9	11	10	10	8		13	14
44	10	11	8	9		8	9		14	17	19	10	8		7	11	10	13	12	17	17	17
45	9	10	10	12	14	12	16	17		18	18	10	11	13	11		11	14	18	17	18	17
46	11	14	12	14	15	12	13	14		16	16	10	11	13		13	11	10	13	13	14	13
47	10	13	12	13	12	10	12	13	12	15	23	12	12	13	12	12	11	12	12	13	14	16
48	8	12	10	9	12	09	10	10	13	13	13	9	10	11	9	11	8	11	11	12	13	13
49	7	8	8	11	11	11	14	11	18	20	30	12	11	12	12	15	13	13	13	14	16	43
50	12	11	13	15	12	11	14	13	13	15	73	10	12	12	12	14	12	14	13	13		15
51			12	11	13	11	12	12	13	12	13	10	11	11	11	17	12	13	14	12	12	13
52	14	14	11	13	12	11	13	14	15	14	15		12	20	14	14	12		14	14	14	13
53	14	13	14	15	15	13	14	16	15	15	18		14	15	14		15	12		17	17	
54	13	15	14	15		15	18	16	17	18	17	15	16	17	15	14	18	18	18		17	18
55	14	17	20	17	17	17	18	17		17	16	17	14	16	15	15	16	16	16	16	15	16
56		18	15	14		18	16	15	15	19	17		16	14	16		15		14	13	15	15
57	13	14	14	16	15	13	15	13	18	15	15	14		14	13	14	15	14	14	12	14	14
58	11	16	14	12	12	13	12	13	14	13	14			13	11	14		11	11		11	13
59	12	13	12	12	13	15	15	15		14	15	22	12	11	15	12	13	12	16	13	16	16
60	10	11	9	9	13	12	13	15	14	14	15	10	9	8	11	10	9	11	13	13	13	
61	7	9	9	8	11	5	6	10		11	12	8	8	9	5	11	2	6	8	8	7	
62	8	9	6			14	13	11	12			9	8	8		11		15	15		15	
63	14	9	10		11	14		14	13	14	17		13	14		15	20	16	16	16	13	14
64	12		13		14	16	15	16	15	20	22		12	10		12	12	12	15			14
65		8	9		9	10	10	10	11	11	15		7	6		8	9	14	14	13	13	14
66	8	7	7	7	7	15	12		13	15	17		6	6	6	6	9	12	15	15	16	15

67	4		8	6	7	7	10	9	14	15	18		7	6	7	6	6	10	9	15		15
68	5					15	15	17	15		17	15		8	15	12	15	18	17			17
69			8	13	16		16	14					10	11	11	13	14	15	18	19		18
70			10	13	10	16	15		15	17	17	11	14	16	14	17	17		17	16	16	17
71	13			16	17	16	15	17	18	18	17	16		17	18	16	16	17	18	16	14	17
72	14	16	16	14	15	16	17	15	16	15	14	15		14	14	15	15	16	15	14	14	15
73	14	14	16	14	18	15	13	14	15	14	14	13	14	13	14	14	14	13	14	14	14	15
74		13	13		14	19	17	15	16	16	19	16	16	17	15	18	15	16	20	19	19	138
75	15	18	17	15	16	15	18	17	18	20	38		16	16	15	17	16	16	17	18	21	48
76	14	18	16	14	16	17	19	17	19		19	10	13	16	12	13	13	16	16	14	16	20
77	6	6	9	12	12	14	16	17	16	14	18	14	16	14	14	17	18		17	16	15	16
78	15	17	16	17	16	16	16	16	16	15	16	13	17	15	14	18	15	14	15	15	17	17
79	15	14	14	16	15	16	15	15	15	16	15	16	15	16	16	15	16	16	16	15	16	16
80	15	16	14	15	14	14	15	17	16	15	16	14		15	14	16	16	15		17	14	16
81	12	15	13	13	13	15	14	17	17	14	15	12	14	13	13	15	14	17	18	20	22	26
82	14	14		16	16		17	19	21	23	25	15	16	16	16	16		21	24	21	26	20
83	15	16		14	16	15	18	21	22	22		12	14		13	18		16	17	21	19	20
84	14	12	14	13	13	15	13	16	13	14	16	11	13	13	12	14	12	12	14	13		13
85	9	8	8	9	12	12	15	14	13		15			9	8	11	8	14	12	12		14
86	9	11	8	10	10	9	9	12	13	12	14	6	10	9	8	11	8	13	12	12	13	13
87		9	9	9	11	14	14	13	13	14	14	9	10	8	9	9		9	14	15	16	17
88	14	14	13	15	13		13	12	14	15	15	18		12	19	12	14	12	13	16		15
89	14	14	14	16	14	13	14	15	15	17	19	11	16	16	12	12	14	13	13		16	18
90	6	5		8	13	11	13	13	16	17	17	9		5	11	10	12	15	12		16	16
91	13	13	14	14	13	14	14	14	15	15	17	17	15	16	23	13	29	14	14	14	16	14
92	9	13	12	10	17	12	13	19	21	15	16	7	9	9	8	12	9	14	12	15	15	17
93		15	12	16	9	16	15		14	15	14	12	12	15	11	15	12	14	14	15	16	
94	12	11	12	13	13	11	14	15	16	15	16		11	12	11	13	12	11	15	15	15	16
95		14	12	16		14	13	16		16	14		12	12	15	13	15	13	14	15	15	13
96	13	15	14	15		15	15	15	13		12		16	15	15	13	14	16	16		13	14
97	11	14	14		14	16	13	14	14	19	19	13	14	14	15	18	16	17	18		18	14
98	15		16	15	18	16	16	17	17	16	17	16	13	14	18	16	15	16	16		16	16
99	15	14		16	15	13	13	13	15	15	15	15	13	12	16	14	15	14	15	16	13	16
100		13		14	13	14	15	15	14	14	15	10		12	13	14	14	13	12	14	14	14
101	16	10	8	11	11	13	9	11	10		13	17	12		14	11	15	13	8	11	14	10
102	13	13	13	13	12	13	14	14	12	12	12	19	15	15	14	14	16	15	14	14	13	15
103	12	12		8	11	14	13	14	12	14	15		14		13		13	14	15	12	15	15
104	13	13		12	19	14	12	15	15	14	15	12	14	17		15	13		13	13	13	12
105	13			14	12	14	13	13	12	12	12	13	12		14	12	12	11	12	13	12	14
106	14	15	13	13	11	12	13	13	14	13	13	13	13	13	13	13	13	10	16	15	13	13
107	13	16			12	12	14	11	12	12	12	13	13		15	12		10	13		13	14
108	10	11		12	13	11	13	13	12	13	15	12	15	11	12	11	11	13	15	15	14	16
109	9	11	9	11	12	11	11	16	15		15	9	10	11	10	12	7	11	14		16	16
110	7		10	6			10	11	12	12	11	9	10		6	15		9	13	11	10	11
111			13	12	13	11	12	12		12	13	9		10	13	11	10	11	15		17	18
112				13	11	13	12	15	15	15	16	11				13	12	13	14		17	18
113	11				13	13	14	17	16	17	17	12				15	14		14		16	16

Table 3. (Contd)

Local day	Morning samples												Evening samples									
	OK	TU	UM	IC	CO	CN	OM	DS	AL	RS	MS	OK	TU	UM	IC	CO	CN	OM	DS	AL	RS	MS
114	12				16	13	13	14		17	16	15		14		15	14	14	16	15	15	13
115	14		12		14	10	12	14	12	13	13	14		12		13	12		13	13	12	13
116	11	16	12	12	11	12	12	11	12	12	12	10	11	12	11	12	11	13	12	13	11	
117	9		10	11	12	7	9	10	9		11	15		19	9	13	10	9	11	9		9
118	11		13	12	15	11	8	11	11		12	11		17	7	14	9	9	11	8		16
119	6			12	10	16	16	12	11	15	16	7			14	8	18	16	18	16	17	19
120	11		11	13	16	14	15	15	14	14	14	13		15	13	14	14	11	13	13	13	14
121	7		14			13	11	12	12	16	14	8			12	14	13	13	14	14	15	12
122	8		11		13	8	14	12		12	12	9		8		13			15		16	16
123	13				15	17		17	16	19	18	14				17			18	17	17	18
124	13		15		17	15		17		15	18	14		15		17	16		18	17	17	17

Blanks indicate missing data. Samplers are identified by the first two letters of their abbreviation.

3. TRANSPORT AND DISPERSION MODEL

The model used to calculate concentrations was adapted from a model developed by Draxler and Taylor (1982) to study the effects of wind shear on a pollutant puff. The effect of wind shear on dispersion is obtained by dividing the vertical extent of the puff within the mixed layer into 300 m sublayers at the beginning of each night. Each layer is tracked by means of a separate trajectory. Vertical mixing is resumed during the next day and subsequent days. New subdivisions occur each night.

The concept of representing the wind-shear induced dispersion of a puff by dividing it into a finite number of subpuffs is similar in some respects to the methods used by Sheih (1978), Henmi (1980) and Samson (1980).

The computer wind shear model used here was designed to simulate the growth of a pollutant cloud in the boundary layer following a technique suggested by Pasquill (1962). From the analysis of several medium range dispersion experiments, Pasquill found that when "effective vertical mixing is present, the tendency for a cloud of particles to be sheared is quite strikingly removed . . . ". However, at night during stable conditions, he found that "the distortion of the cloud can proceed without opposition, yielding horizontal displacements which are potentially effective at other levels and merely require the revival of vertical mixing in order to become actually effective".

3.1. *Model structure*

The model is essentially a Lagrangian puff trajectory model. However, to compute efficiently the trajectories of many more puffs the calculational procedure was indexed to a one degree latitude–longitude grid and 10 vertical coordinates of 300 m increments. The position of meteorological stations and the reported winds, the location of each puff after each advection step, and the receptors for air concentration calculations were all indexed by grid coordinates. In this way, advection and air concentration calculations could be performed quickly without having to test all the data each time step. Note that this is not a grid type model. Data are not interpolated to a grid; only the position of significant elements of the calculational procedure is given in grid coordinates. The resolution of position of each puff is to the nearest hundredth degree of latitude and longitude.

3.2. *Advection*

Pollutant puffs are released every 3 h. Each puff has a different mass consistent with the emission rate given in Table 2. The trajectory of each puff is constructed of 3 h advection segments using a one-step Euler numerical integration. In the United States the 00Z (Z—Greenwich Mean Time) wind field is used for daytime (12Z to 00Z) tranport and the 12Z wind field is used for night-time (00Z to 12Z) transport. The use of morning and evening soundings to represent the

previous 12 h is preferable to centering the time interval because this is a more realistic representation of the winds in the boundary layer during the day- and night-time regimes in the United States.

Only rawinsonde data from the observing times of 00Z and 12Z are used. No time interpolation is performed. The rawinsonde nearest to the puff position is used for the calculation. The distance travelled each time step is equal to the vector average wind in the layer multiplied by the advection time step. Puffs are advected for the entire model run or until they pass off the computational grid. The rawinsonde data are available for the United States on magnetic tape from NOAA's National Climatic Center, Ashville, NC 28801, U.S.A.

3.3. *Vertical mixing and wind shear*

Wind shear effects are incorporated by applying the diurnal differences in vertical mixing to the winds in the vertical layer used to calculate advection. No vertical mixing is assumed at night and complete mixing is assumed during the day within the mixed layer below the temperature inversion determined at every rawinsonde station each day following the method of Heffter (1980).

If the release is at night, the puff is constrained to the lowest transport layer (0–300 m). Releases during the day are assumed to mix to the top of the mixed layer instantaneously. During the next nocturnal period (00–12Z), when no vertical mixing is assumed, a puff is split into 300 m sublayers within the previous mixed layer. The interval of 300 m was chosen for the maximum vertical resolution because the wind data are reported at approximately that interval. After a puff is split at the beginning of the nocturnal phase, the layers are followed as separate trajectories for all subsequent calculations. During the next daytime phase, the elevated layers become fully mixed to the surface and affect air concentrations. The mixed layer during subsequent daytime periods may not be as large, and hence layers may be trapped above the new mixed layer. These layers will be advected with the appropriate wind at that level and will not affect surface air concentrations unless the mixed layer the next day reaches that height.

3.4. *Surface air concentrations*

The horizontal spreading of the vertical layered pollutant puffs simulates the wind shear effect. However, turbulent diffusion still plays a dominant role in spreading the pollutant puff during the first 24 h before the dispersion due to wind shear begins to exceed the turbulent horizontal dispersion. The dispersive effect of the wind shear on the pollutant puff is cumulative, but only in increasing the puff's horizontal extent each night. Turbulent puff growth is assumed to occur at all travel times. The rate of turbulent puff growth is assumed to be the same as found by Heffter (1965) where the horizontal standard deviation (S. D.) of concentration is given by a linear growth, Sigma $= 0.5T$, where Sigma is in m and T, the travel time, is given in s. Heffter's curve represents the average of many different experiments. However, the data used were only those where a distinctive Gaussian plume could be measured. Therefore, those situations in which considerable wind shears might have spread out the pollutant were not included, suggesting that this might be a good approximation of the turbulent diffusion only.

For the purpose of calculating concentrations, concentrations are assumed to be uniform across a disk defined by a diameter of 4 Sigma. The air concentration in this disk is then just the total emitted mass of the pollutant, divided by the area of the disk, times its depth. During the daytime, for a puff within the mixed layer, this depth is equal to the mixed layer. At night, only puffs within the 0–300 m layer contribute to surface air concentrations. The depth in this case is 300 m.

Concentration calculations are performed for all grid locations. Each puff contributes the same concentration to each grid intersection within the puff diameter at each advection step.

3.5. *Computational considerations*

Trajectory calculations, although time consuming due to the daily exponential increase in the number of trajectories, are not unduly expensive. Computer time and core requirements are less than that of the model developed by Heffter *et al.* (1975) applied to the same calculational period. Several features of the computer code, in addition to the indexing by grid position, are used to increase computational efficiency.

(1) Sines and cosines are pre-computed and stored by whole degrees (the resolution of the wind directions); (2) no space or time interpolation of meteorological data is performed; (3) the masses of two or more puffs at the same grid coordinates are combined, and then any (4) individual puffs whose mass has become too small to affect the air concentrations are eliminated.

3.6. *Overview*

The significant difference between the model presented here and others that incorporate wind shear effects lies primarily in the assumption of subdividing the entire daytime mixed layer, during the nocturnal phase, into separate trajectories. This permits, for instance, layers above the surface to be advected at high speeds in a nocturnal jet, while lower layers near the surface proceed at much slower speeds. The tracer gas measured at 600 km, as reported by Ferber *et al.* (1981), must have gone through a similar cycle. The tracer from the 3 h release in the afternoon was measured at the 600 km arc within 12 h after travelling in a strong nocturnal jet. Tracer material, which was measured on the sampling arc for the next 18 h, must have travelled with the slower surface winds. However, the situation is not entirely straightforward since the tracer first arrived at the arc at night and was measured

at the surface. This suggests that strong wind-shear induced turbulence between the surface and the jet permitted the tracer to mix downward. However this degree of detail can not be simulated in this type of Lagrangian trajectory model, since the rawinsonde times (00 and 12Z) do not reflect the time of the maximum nocturnal jet.

Measurements of a smelter plume to distances of 1000 km by Carras and Williams (1981) showed that the horizontal dispersion was strongly influenced by nocturnal wind shears. They found that they could model the measured plume widths to within 30% when the plume from the previous day was tracked by separate trajectories at about 300 m height increments in the nocturnal boundary layer. Further, they found that during the daytime the vertical mixing was intense enough to distribute the pollutant to the top of the mixed layer within 30 min.

4. ANALYSIS TECHNIQUE

Analysis of measured and calculated Kr-85 concentrations will proceed under a somewhat different approach than in previous investigations. No attempt will be made to determine an exact background concentration, since the variations in background will be found to be at least the same magnitude as the Kr-85 plumes from Idaho. The analysis method will reflect the following assumptions:

(1) the time series of the fluctuations of calculated and measured concentrations, however small, will be the primary measure of model performance;

(2) both measured and calculated concentration fluctuations will be periodic with a similar distribution of variance in the frequency spectrum, if the model has any skill and

(3) random noise, due to model error, variation in sampler efficiency, laboratory analysis error, or due to the nature of atmospheric turbulence, will not be frequency dependent.

The analysis procedure (which uses the Statistical Analysis System, SAS Institute Inc., P.O. Box 10066, Raleigh, NC 27605, U.S.A.) begins by first decomposing each time series into sine and cosine series using a Fast Fourier Transform. The square of the coherence of the measured and calculated time series, which is similar to a correlation squared except it is a function of frequency, is then applied as a weighting factor to each frequency-dependent sine and cosine term when the measured and calculated time series are inverted by means of an inverse Fourier transformation. In this way variance in uncorrelated frequencies is filtered out.

In summary, the analysis procedure applied to both measured and calculated data consists of two parts:
(1) Decomposition of the time series:

$$A_k = 2N^{-1} \sum_{t=1}^{N} X_t \cos(W_k t)$$

$$B_k = 2N^{-1} \sum_{t=1}^{N} X_t \sin(W_k t).$$

(2) Reconstruction of the time series from the coefficients:

$$X_t = \overline{X} + \sum_{k=1}^{N/2} [A_k C_k \cos(W_k t) + B_k C_k \sin(W_k t)],$$

where X_t is the time series of N data points and C_k is the square of the coherence of the calculated and measured time series with frequency W_k, given by

$$W_k = 2\pi k N^{-1}$$

and k varies from 1 to $0.5N$.

The reconstructed time series will be smoother, and the variance in uncorrelated frequencies is reduced. Examples of these effects will be shown in the next section. This method tends to enhance some periodicities in the measured and calculated data and reduce others. The basic structure of each time series remains unaffected. These techniques would not be necessary when plume concentrations are well above background. However, to compare models with the midwest Kr-85 data, special techniques must be applied that would not ordinarily be attempted.

The reconstructed, filtered time series are then compared by standard linear regression procedures. In addition to the slope of the regression line of calculated on measured concentrations, the ratio of the S.D. of calculated to the S.D. of measured concentrations is used as a measure of overall model performance in terms of over- or under-calculation. The S.D. should be a good measure ofplume amplitude in the filtered series, since other variances have been reduced. This ratio can be compared directly with the slope from the regression estimate. The higher the correlation the closer the slope should be to the ratio of the S.D.s.

5. TESTING MODEL CALCULATIONS OF Kr-85

Shear model calculations were performed for the period of Kr-85 emissions from Idaho shown in Table 2. Puffs were started with the appropriate mass of Kr-85 each 3 h. No puffs were emitted when the emissions were zero. Actual rawinsonde observations for the calculational period were used for advection and mixing depth calculations. Average concentrations were computed to coincide with the sampling interval at the 11 sampling sites for 132 consecutive samples. These calculated values were then compared to the measured data shown in Table 3 after a two-sample running average was performed to smooth some of the noise.

5.1. *Individual station results*

A summary of model performance by station, before and after the spectral filter was applied, is shown in Table 4. Primed quantities were calculated after filtering. M and C refer to measured and calculated means

Table 4. Statistical summary of model performance by station

Station	M	σ_m	C	σ_c	$\frac{\sigma_c}{\sigma_m}$	$\frac{\sigma_{c'}}{\sigma_{m'}}$	S	r^2	S'	$r^{2'}$
MSP	13.7	0.91	.22	.28	0.30	0.34	−0.04	.02	−0.07	.04
RST	13.5	0.26	.23	.31	1.2	1.0	−0.11	.01	−0.36	.12
ALO	13.4	0.23	.25	.33	1.4	1.4	−0.25	.03	−0.46	.11
DSM	13.4	0.23	.28	.35	1.5	1.4	−0.10	.00	0.12	.01
OMA	13.3	0.22	.36	.48	2.1	1.7	0.39	.03	1.2	.50
CNK	13.3	0.27	.34	.47	1.7	1.6	0.41	.06	1.2	.59
COU	13.3	0.23	.20	.24	1.0	1.3	−0.03	.00	−0.13	.01
ICT	13.2	0.31	.28	.35	1.1	1.1	0.48	.18	0.83	.58
UMN	13.2	0.28	.17	.23	0.82	.92	0.25	.10	0.60	.43
TUL	13.2	0.26	.22	.28	1.1	1.2	0.48	.20	0.98	.73
OKC	13.2	0.28	.20	.28	1.0	1.3	0.36	.13	0.95	.57

M, measured mean; σ_m, measured S.D.; C, calculated mean; σ_c, calculated S.D.; ', results after filtering; S, slope of calculated on measured from linear regression and r^2, correlation squared.

and their S.D.s are denoted by σ_m and σ_c, respectively. From the linear regression the correlation squared is given by r^2 and the slope of C on M by S.

The important assumption in the analysis of these data is that the concentration fluctuations rather than the mean concentrations are indicative of model performance. This assumption may not be appropriate for all situations. However, the dispersion properties of the atmosphere and the large distance from source to receptor lead to large peaks as well as periods of zero concentration. The highest calculated mean concentration (Table 4), which is at OMA, does correspond to the highest calculated S.D. Similarly the minimum mean and S.D.s are at UMN. Except for MSP, which will be discussed later, the ratio of σ_c/σ_m before or after the filtering, tends to be within a factor of 2. In the southern stations (ICT, UMN, TUL, OKC) the match is exceptional, within 30%. The good match between measured and calculated values indicates that the overall magnitude of the fluctuations in the time series of concentrations is similar and the model is not over- or under-calculating. However it remains to be proven whether the fluctuations in measured concentrations can be attributed to the Idaho source and how well they are correlated to the model calculations.

The last four columns of Table 4 give the slopes and correlations of calculated on measured concentrations before and after filtering. The slopes should be similar to the ratio of the S.D.s. However large scatter of measured to calculated values introduces bias in the slope of a regression estimate. The lower the correlation the larger the bias. Note that the slopes of the filtered data most closely match the ratio of $\sigma_{c'}/\sigma_{m'}$ when the correlation is large. The largest correlations are for stations located in the south. Figure 2 shows the filtered correlations and illustrates a spatial relationship not as apparent from Table 4. Not only does the correlation decrease to the north but to the east as well.

The model did not perform as well at the stations to the east probably in part due to the lower calculated values at these sites. Note from Table 4 that COU and UMN had considerably lower calculated concentrations than the stations to the west (CNK and ICT) at approximately the same latitude. These lower calculated values suggest that the Kr-85 plume from Idaho could have been below some critical value so that it was within the noise level of the measurements. The less satisfactory model performance to the north will be discussed in the next section.

5.2. *Other sources of Kr-85*

Ferber *et al.* (1977) suspected a local source of Kr-85 near MSP. The much larger σ_m at MSP than RST and ALO indicates that something other than background fluctuations are being measured, since background fluctuations should not have such a large spatial gradient. To investigate this further, the M and σ_m of the Kr-85 concentration measured at MSP are shown in Fig. 3 as a function of wind direction (in 10° bands) during each sampling interval for the entire sampling period (February to May). The reported 3 h surface wind at MSP was used. Peaks from two distinct sectors are evident, at azimuths of 210–230° (11 samples) and 300–320° (34 samples). The concentration fluctuations from these two sectors are much larger than would be expected from the Idaho source or from just natural variability. No other sampler measured variations of this magnitude.

There are sources of Kr-85 that can never be accounted for properly. For instance, boiling-water nuclear power plants have routine releases of noble gases, including Kr-85. Although such releases are very small, at short distances the concentrations from these sources might just exceed the concentrations from larger more distant sources. To produce such a peak at MSP would require a source on the order of about 1 Ci $(3\,\mathrm{h})^{-1}$ if it is assumed that in a 30° sector, the mean excess concentration 50 km from a local source is about 0.5 pCi m^{-3}. Nuclear power plants are located near many of the northern sampling sites, including one about 50 km northwest of MSP. The only power plant near any of the southern stations is in central Arkansas.

It appears that there may be one or more local

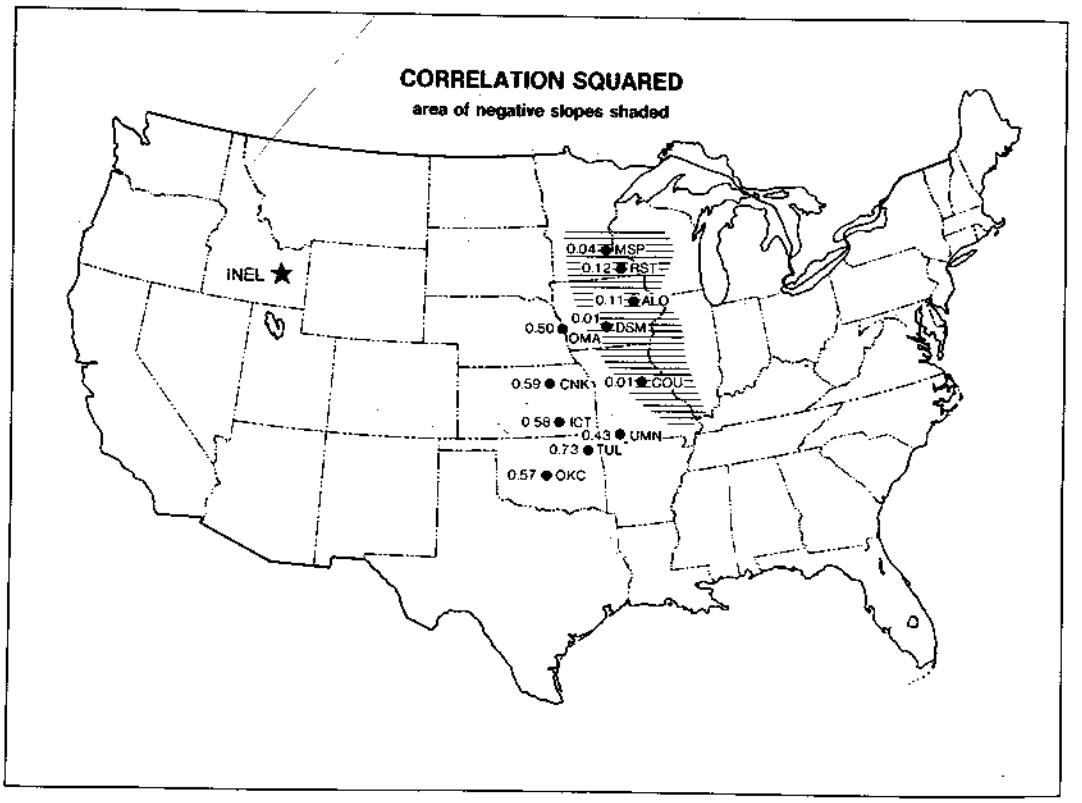

Fig. 2. The correlations of calculated to measured concentrations at the sampling sites for emissions from Idaho.

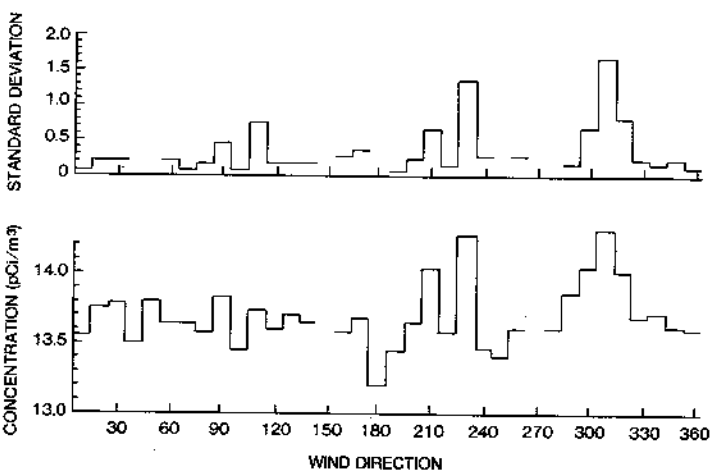

Fig. 3. The mean and S.D. of Kr-85 concentrations (pCi m^{-3}) at MSP shown as a function of surface wind direction at MSP coincident with each sampling period.

sources of Kr-85 near MSP. The effect of these on some of the more distant samplers can be evaluated. Since the actual emissions are not known, nor are they likely to be continuous, the relative contributions of Idaho and the MSP area can be judged by calculating concentrations at the samplers assuming a constant emission from MSP of 1 Ci $(3h)^{-1}$, using the same model for the same period as for Idaho. The calculated concentration S.D.s are shown in Fig. 4. Probably the extent of the area of influence of the MSP source would not exceed the 0.1 pCi m^{-3} isopleth, a fluctuation about half of that calculated from the Idaho source. Therefore, small emissions near MSP will affect concentrations at least at RST and ALO. It is

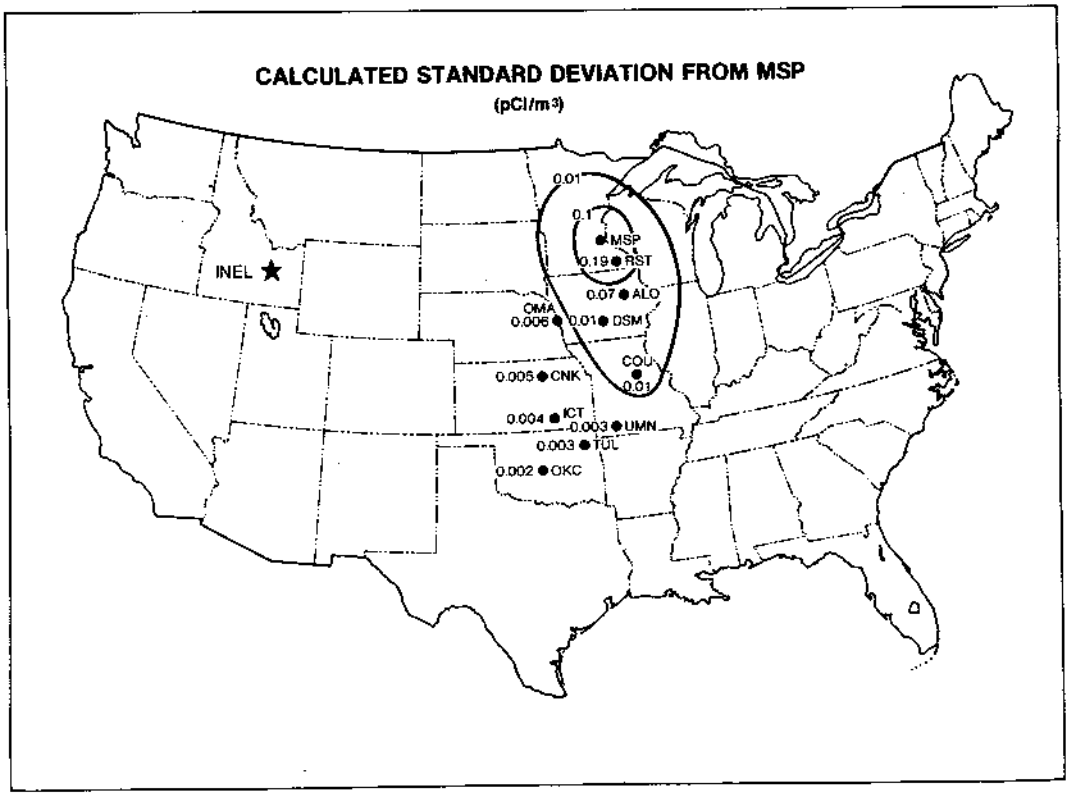

Fig. 4. The S.D.s of calculated concentrations (pCi m^{-3}) for emissions from the MSP area.

conceivable that individual episodes might extend to the 0.01 pCi m^{-3} isopleth. Note that the area of influence of the local source approximately corresponds with the area of poor model performance seen in Fig. 2.

In the next three sections the stations (ICT, TUL, OKC), which had the best performance as demonstrated in Table 4, will be used to illustrate the effect of the spectral filter, investigate the influence of the meteorology on the model calculations and provide sensitivity tests of some of the model assumptions.

5.3. *Example of spectral filter*

The sampling sites that are presumed to be unaffected by complications are combined into one group: OKC, TUL, ICT. The air concentration data from these stations are then averaged together for each sampling period. Averaging data from adjacent stations helps smooth some of the variability and also eliminates the problem of missing data, since at least one station in the group usually has a measurement. The group averaged data, as before, are then averaged by a one-period running mean. These data are then subject to analysis.

In the previous section the effect of the spectral filter was not examined in detail because of the complications that were evident in the data at many of the sampling sites. The grouped data provide a more consistent and limited data set for further model testing. The spectra of measured and calculated values are shown in Fig. 5. The spectrum is the distribution of the fraction of the total variance of concentration as a function of frequency ($f = 0$ to π). The period of any frequency is given by $2\pi/f$ times the data collection interval (1/2 day). Both calculated and measured

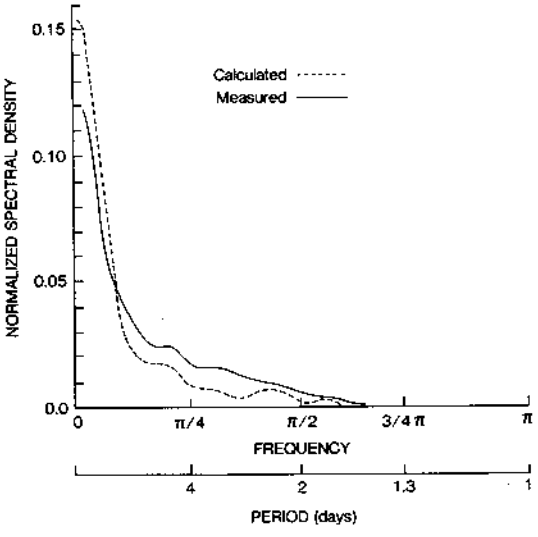

Fig. 5. Concentration spectra for calculated and measured data shown as fractional variance by frequency (0 to π) and period.

distributions are remarkably similar. Each show increasing variance at lower frequencies. Low frequency variance could be an indication of the seasonal variation of Kr-85 background. This would be included at the lower frequencies. For these stations the low frequency variation is also indicated by the model, which implies that most of the Kr-85 concentration fluctuation must come from Idaho since no background concentration is modeled.

The coherence squared between the calculated and measured data is shown in Fig. 6. Coherences above 0.28 are significant at the 95% level. Both low and high frequencies show increasing coherence. A variable band with periods of 2–4 days also shows higher coherence. When the coherence is used as a filter to reconstruct the calculated and measured time series, those frequencies with higher coherence receive greater weight. This effectively filters much of the noise and random error in both series. The scatter diagram of the raw ($r^2 = 0.22$; $S = 0.52$) and filtered ($r^{2\prime} = 0.67$; $S' = 1.0$) data are shown in Fig. 7. The scatter has been considerably reduced and the slope of the filtered series is much closer to what is expected from the ratio of the S.D.s of the two series (1.25).

To demonstrate that the filtering method does not introduce excessive artificial correlation, the original and filtered time series are shown in Fig. 8. Note that as in Fig. 7, the mean has been removed from both measured and calculated concentrations. Although the filtering does reduce the total variance (over 50%), the relationship between the measured and calculated is not affected. For instance the day to day trend between calculated and measured concentrations for days 75–105 is remarkable even before the filter is applied. Neither this relationship, nor the less satisfactory performance before day 75 and after day 105, is altered in the filtered series. The lower frequency variability, in which the model also performs well, is especially enhanced.

5.4. *Meteorological influences on transport and dispersion*

Given all the complications of the Kr-85 data discussed so far, it is difficult to understand why the model calculations for the southern group of stations (as illustrated by Fig. 8) were so good. It is possible that airmass variations in background are responsible for the higher correlation in the south, since the orientation of Idaho relative to the southern stations is more in line with what the flow would be when airmass changes occur (NW behind fronts) to give higher background Kr-85.

A comparison of the peaks and troughs shown in Fig. 8 with daily weather maps does show a pattern. The troughs correspond with southwest flow before frontal passage and the peaks with northwest flow behind the cold front. It is possible that the Idaho plume can be masked by airmass background changes, since they would be in phase. In addition, measured S.D.s were larger at the sampling stations during the non-emission period than when the Idaho source was emitting. This indicates that changes in concentration due to airmass can be expected to be of the same magnitude or even larger than those from the Idaho source.

To further test how much of the apparent model skill might be coincidence, concentration calculations for the first month of sampling (the non-emission period), assuming a constant emission from Idaho, produced a correlation (after filtering) between measured and calculated concentrations of 0.0 as

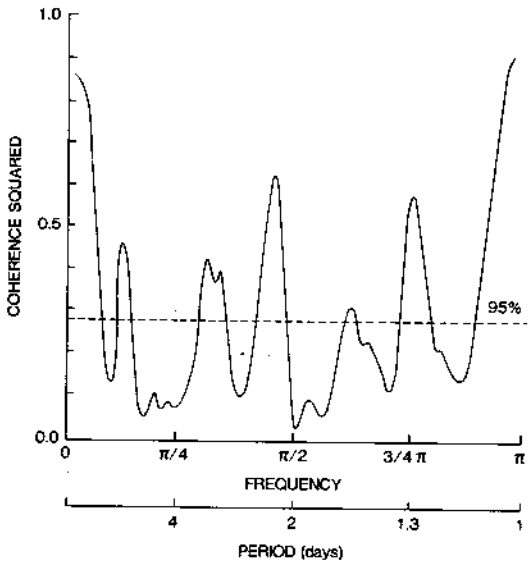

Fig. 6. The coherence squared of measured to calculated concentrations by frequency and period.

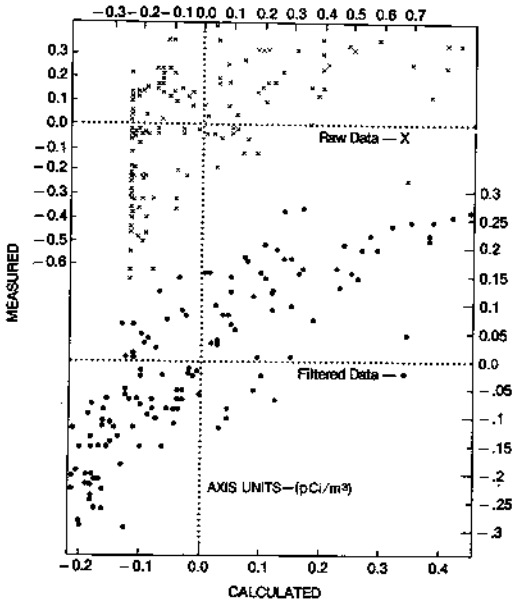

Fig. 7. The scatter of calculated to measured concentrations before and after filtering. Note the change in scales.

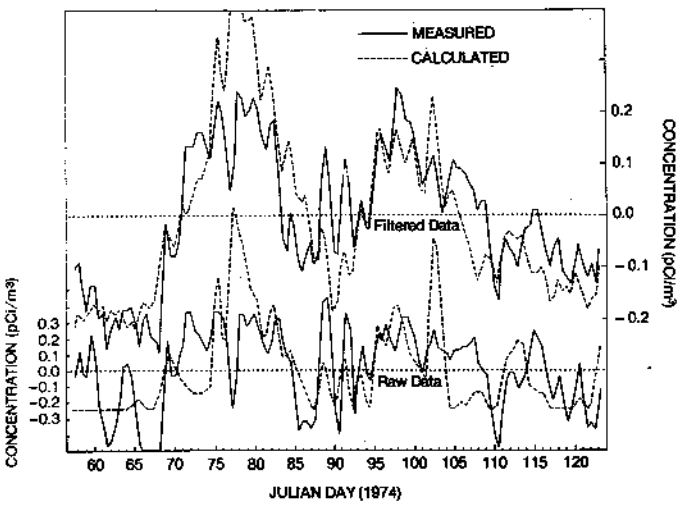

Fig. 8. The time series of calculated and measured concentrations before and after filtering. Note the change in scales.

compared to $r^{2\prime} = 0.67$ during the emission period. Even with the complications of a variable background due to airmass changes, the model calculations during the emission period showed a good correlation with the measurements.

Furthermore, when test calculations were performed during the emission period using an average emission for the entire period (equal to the average of the actual emissions), the correlation was not as large ($r^{2\prime} = 0.57$) at the southern stations. This sensitivity to emissions indicates that the good agreement between measured and calculated concentrations was not entirely fortuitous. Therefore it is still possible to use the Kr-85 data, at least at the southern stations, for further model verification and diagnostic purposes.

The flow needed to transport Kr-85 to the southern stations is usually very straight and uncomplicated, consisting of a northwest flow through a uniform airmass. The accompanying upper air trough tends to be to the east of the sampling sites. Kr-85 flow to the northern sites usually occurs with more complicated regimes, involving some kind of zonal flow. It appears that this kind of situation, typical of what would be necessary to transport Kr-85 from Idaho due east, is much more difficult to model without considering other variables such as airmass properties or vertical motions. Neither of these is considered in the wind shear model used for the calculations.

5.5. *Wind shear model sensitivity*

It would be interesting to test some of the assumptions of the model: this includes linear puff growth due to turbulence about each wind-shear generated subpuff, the instantaneous vertical mixing during daytime transport (12 to 00Z), and the assumption that the shear-generated dispersion was responsible for some of the lower calculated concentrations.

Three test calculations were performed using the southern group of stations. In one the puff diameter was assigned the constant value 100 km (the approximate grid spacing), so that all the additional horizontal dispersion would be only due to puff division from wind shear. The second set of calculations was performed so that the elevated subpuffs from the previous night cycle were not fully mixed until the second daytime advection step (15 to 18Z). During the first advection step the puffs were assumed to be mixed only halfway to the surface or aloft. In the third set of calculations the puffs were not permitted to separate during the nocturnal cycle, so that all the calculated diffusion was due to turbulence. The standard results were from the model as described in section 3.0. The calculational results are summarized in Table 5.

Although the change in correlations is not especially dramatic for the three test cases, a significant change in the slope occurred when no turbulent diffusion or shear diffusion was assumed. These overcalculations indicate that the shear dispersion as well as the turbulent dispersion must be included to properly model concentrations at these distances. Draxler and Taylor (1982) found that the wind shear begins to dominate the horizontal dispersion after about 24–48 h travel. It appears that the midwest Kr-85 data reflect travel times during the transition period from turbulent- to shear-dominated dispersion. Calculated concentra-

Table 5. Slope (S'), correlation squared ($r^{2\prime}$) and ratio of the S.D.s ($\sigma_{c'}/\sigma_{m'}$) for sensitivity tests on south group with the standard model (section 3.), no turbulent dispersion, slower vertical diffusion and no shear dispersion

	Standard model	No turbulent	Vertical diffusion	No shear
S'	1.0	1.7	1.0	1.4
$r^{2\prime}$	0.67	0.63	0.75	0.66
$\sigma_{c'}/\sigma_{m'}$	1.3	2.1	1.2	1.8

tions at larger distances should not be as sensitive to the turbulent diffusion assumption.

A slight improvement was obtained when slower vertical mixing was specified. However, the change does not appear to be significant enough to warrent modification of the model at this time. When additional verification data are available more refined vertical diffusion modeling will most likely be necessary.

6. SUMMARY

The 1974 midwest Kr-85 experiment, although complicated by near-background plume concentrations and contamination from local sources, can still be used to test the transport and dispersion of long-range models. Sampling stations to the south and west were unaffected by local sources or indistinct plumes masked by background fluctuations. Improved resolution was obtained by filtering undesired noise from both measured and calculated concentrations. The filtering resulted in unbiased regression estimates of the slope of calculated on measured concentrations.

Previous modeling efforts with these data showed considerable over-calculation of ground concentrations. A model developed to reflect the effects of wind shear was successful in producing much lower calculated concentrations 1500 km from the source. Calculated small-amplitude concentration fluctuations compared favorably with the measured data.

Acknowledgement—This work was supported by the U.S. Air Force Technical Applications Center.

REFERENCES

Carras J. N. and Williams D. J. (1981) The long-range dispersion of a plume from an isolated point source. *Atmospheric Environment* **15**, 2205–2217.

Draxler R. R. and Taylor A. D. (1982) Horizontal dispersion parameters for long-range transport modeling. *J. appl. Met.* **21**, 367–372.

Ferber G. J., Telegadas K., Heffter J. L., Dickson C. R., Dietz R. N. and Krey P. W. (1981) Demonstration of a long-range atmospheric tracer system using perfluorocarbons, NOAA Tech. Memo ERL ARL-101, Silver Spring, MD, U.S.A.

Ferber G. J., Telegadas K., Heffter J. L. and Smith M. E. (1977) Air concentrations of Krypton-85 in the midwestern United States during January–May 1974. *Atmospheric Environment* **11**, 379–385.

Heffter J. L. (1965) The variation of horizontal diffusion parameters with time for travel periods of one hour or longer. *J. appl. Met.* **4**, 153–156.

Heffter J. L. (1980) Transport layer depth calculations, *Second Joint Conf. on Applications of Air Pollution Meteorology*, New Orleans, Am. Met. Soc., 787–791.

Heffter J. L., Taylor A. D. and Ferber G. J. (1975) A regional–continental scale transport, diffusion and deposition model, NOAA Tech. Memo ERL ARL-50, Silver Spring, MD, U.S.A.

Henmi T. (1980) Long-range transport model of SO_2 and sulfate and its application to the eastern United States. *J. geophys. Res.* **85**, 4436–4442.

Pack D. H., Ferber G. J., Heffter J. L., Telegadas K., Angell J. K., Hoecker W. H. and Machta L. (1978) Meteorology of long-range transport. *Atmospheric Environment* **12**, 425–444.

Pasquill F. (1962) Some observed properties of medium scale diffusion in the atmosphere. *Q. Jl R. met. Soc.* **88**, 70–79.

Samson P. J. (1980) Trajectory analysis of summertime sulfate concentrations in the northeastern United States. *J. appl. met.* **19**, 1382–1394.

Sheih C. M. (1978) A puff pollutant dispersion model with wind shear and dynamic plume rise. *Atmospheric Environment* **12**, 1933–1938.

Sulfur in the Atmosphere (1978) *Proc. Int. Symp.* Dubrovnik, Yugoslavia, 7–14 September 1977. *Atmospheric Environment* **12**, 1–796.